Reconstruction of Measured Antenna Patterns and Related Time-Varying Aperture Fields

J. Martí-Canales and L. P. Ligthart

***Abstract*—In this paper, the authors present a method to reconstruct measured antenna radiation patterns and their related time-varying aperture fields. The method is based on a model that accounts for the measurement scenario and the antenna radiation characteristics through its radiation centers. The inputs to the model are radiation pattern measurements over a certain bandwidth. Solving the model provides the number of radiation centers, the patterns coupled with each radiation center, and the time delay at which these patterns would be measured. With this information one can reconstruct the measured pattern and retrieve the time-varying aperture fields of the antenna. The latter also provides a diagnostic tool for complex radiating structures. The method and the model are validated with measurements performed in a compact range of two spaceborne antennas.**

***Index Terms*—Antenna measurements, time domain holography.**

I. Introduction

The source of radiation in antennas is a permanent question in electromagnetics. Different approaches are available in the literature, but all authors coincide about radiation being actually produced at privileged locations on the antenna [1]–[3], i.e., the radiation centers, and their importance for further optimization of existing designs [4], [5]. The actual physics behind each radiation center depends on the antenna itself, and its analytical determination is not straightforward. The concept of radiation center is here exploited in the context of antenna measurements.

In order to improve the accuracy of antenna measurements, one needs to account for the number of contributions in the measured pattern, i.e., perturbations and actual responses. The pattern measured at the terminals of an antenna under test is affected not only by the multipath environment in the test range but also by the radiation characteristics of the transmitting and receiving antennas. A similar situation is observed in other scenarios, such as in mobile communications, on large spacecraft, or even at the international space station.

The outgoing radiation power is affected by both the radiation pattern of the transmitting antenna and the presence of surrounding objects in between the transmitting and the receiving antennas. In this way, the receiving antenna is immersed in a multipath environment, where incoming plane waves would arrive with different time delays that are proportional to the electrical path followed in their propagation.

In this paper, we present a first-order decomposition of the measurement recorded at the terminals of the antenna under test into several timely spaced contributions. Such contributions arise from the interactions between the radiation mechanisms present in the antenna and the incoming plane waves. Due to limitations imposed by the measurement itself (e.g., finite bandwidth), the capability to discriminate individual radiation mechanisms present in the antenna is further limited. Therefore, each contribution found in the measurement actually arises from the interaction of a plane wave to a combination of radiation mechanisms as produced by the antenna in a given measurement scenario. Each of these combinations is represented by one equivalent radiation center and one coupled radiation pattern. In this way, the method presented in this paper retrieves from a measured radiation pattern the number of contributions or combination of radiation mechanisms, the measurement time delay, and their radiation pattern. This information is finally used to reconstruct the measured radiation pattern.

In order to relate the obtained contributions to the antenna geometry, the authors have extended the time-domain holography presented in [6], [7] to a new time-varying holography obtained from bandlimited measurements. In brief, each radiation pattern coupled with a radiation center is individually transformed back to the aperture of the antenna and further plotted as a function of their time delay. This holography provides a visualization of the time-varying fields, and also a new tool for nondestructive reverse engineering.

To illustrate both the reconstruction and the time-varying holography, this paper also presents results from measurements performed of two different space-borne antennas.

II. Description of the Model

As stated above, the measured radiation pattern at the antenna terminals can be decomposed in a number of timely spaced radiation patterns that are coupled to the radiation centers of the antenna. When added together these patterns reconstruct the original measured radiation pattern.

Let us consider that the radiation pattern is measured over a discrete bandwidth $B = \{f_1, f_2, \ldots, f_M\}$ of M evenly distributed frequencies, with increment Δf. Thus, the expression for the measured pattern at frequency $f_m \in B$ is

$$V_m(\theta,\phi) = \sum_{p=1}^{P} V_p(\theta,\phi,B) e^{-j(m-1)2\pi\Delta f \cdot t_p} + n_m(\theta,\phi), \quad \text{for } m = 1, \ldots, M \quad (1)$$

where $V_m(\theta,\phi)$ is the measured pattern as a function of spherical coordinates at the frequency f_m, $V_p(\theta,\phi,B)$ is the pattern that is measured at the pth radiation center of the antenna, P is the number of radiation centers, t_p is the time delay at which the pth pattern is measured, and $n_m(\theta,\phi)$ is the additional white noise, assumed of zero mean and small variance. It is worth mentioning that the patterns $V_p(\theta,\phi,B)$ are a unique set over the bandwidth B, as will be shown later.

One important consideration is that the model developed is based on measurements taken at the antenna terminals. Thus in the time domain, the measurement is formed by a sequence of timely spaced aspect angle dependent contributions. The individual contributions identified by our model are assumed to be a combination of one or more radiation mechanisms in response to one or more incoming plane waves due to the multipath environment. Because the contributions are measured at the antenna terminals, it is the antenna itself the one that applies the appropriate "algebra" to combine the radiation mechanisms contained in each contribution. In addition, the resultant contributions occur at instances that depend on both the antenna characteristics and the time delays of the incoming plane waves.

The next step is to solve (1) in order to obtain the number of radiation centers and their associated time delays. The authors have chosen the MUSIC algorithm [8], which provides greater resolution than other known techniques that are based on the Fourier transform, e.g., beamforming. Superresolution techniques have extensively been discussed in the literature for processing radar signals, with their main application being the identification of time and direction of arrival of backscattered radar signals. In antenna measurements, the MUSIC algorithm was already used in [9] to reconstruct far field, time-domain antenna measurements in small anechoic chambers. To our knowledge, this is the

Manuscript received June 3, 2002; revised September 30, 2003.
J. Martí-Canales is with the European Space Research and Technology Center, 2200 AG Noordwijk, The Netherlands (e-mail: javier.marti.canales@esa.int).
L. P. Ligthart is with the International Research Center for Telecommunications-Transmission and Radar, 2600 GA Delft, The Netherlands.
Digital Object Identifier 10.1109/TAP.2004.835235

first time MUSIC is applied to retrieve the patterns associated to the radiation centers of an antenna.

The resolving power of MUSIC discussed in [10] limits the applicability of the model above. The main parameters to take into account are:

1) signal-to-noise ratio of the measurement;
2) number of measured frequencies over the bandwidth;
3) the bandwidth itself;
4) the correlation between contributions.

The correlation between contributions can be overcome by applying a whitening process [11], which makes all contributions uncorrelated. Then, the optimum combination of parameters strongly depends on the antenna under test and the test range itself. Based on our own experience, the model can be actually resolved for bandwidths up to 1 GHz, a maximum number of frequencies about 70, and signal-to- noise ratios above 21 dB.

As discussed in Section I, the radiation centers identified with this model result from a combination of one or more radiation centers' being excited by one or more incoming plane waves. Therefore, the obtained time delays do correspond to the centroid of a combined radiation mechanism. The time delays of the various centroids are obtained from the frequency diversity information contained only in a given aspect angle of the measured antenna, i.e., boresight.

The last step in the reconstruction of the measured signal is to compute[1] the radiation patterns coupled to the radiation centers $\hat{V}_p\ (\theta, \phi, B)$. In this step, the entire angular range measured is used, so that the angular dependence is included in the model. The patterns are obtained by minimizing the least square approximation of the difference between the measured and the computed pattern [9]. In this manner, the patterns are a unique set for the reconstruction of the measured pattern over the entire bandwidth. Once these patterns are obtained, the reconstruction at the frequency f_m is performed using the following expression:

$$\widehat{V}_m(\theta, \phi) = \sum_{p=1}^{P} \widehat{V}_p(\theta, \phi, B) e^{-j2\pi f_m \widehat{t}_p}, \quad \text{for } m = 1, \ldots, M. \quad (2)$$

Lastly, in order to retrieve the time-varying aperture fields or time-varying holography, the patterns associated to the radiation centers $\hat{V}_p\ (\theta, \phi, B)$ are individually transformed to the near field as follows:

$$\hat{V}_{\text{aperture},p}(x, y) = \frac{1}{2\pi} \int_{-\infty}^{\infty} \int_{-\infty}^{\infty} \hat{V}_p(k_X, k_Y, B) k_Z^{-1} e^{j(k_X x + k_Y y)} dk_x dk_y \quad (3)$$

where $\hat{V}_{\text{aperture},p}\ (x, y)$ is the spatial field distribution at the aperture of the antenna corresponding to the pth radiation center, and (k_X, k_Y, k_Z) the components of the propagation vector. The resultant aperture fields, a total of P, are then plotted versus time to generate the time-varying holography.

Since the time-varying holography is obtained from a bandlimited measurement, the provided visualization is only related to the bandwidth considered for the model. Therefore, one cannot expect to gain insight into all features of the antenna. This holography is an extension of the direct time-domain holography described in [6], [7] where measured time-domain responses are directly transformed to the near field. In the latter case, the resultant holography contains the features of a much broader spectrum provided by the excitation time-impulse, typically on the order of the first 18–20 GHz. The new approach presents the advantage that the time-varying holography can be also obtained from measurements performed in the frequency domain over a limited bandwidth.

[1]Computer calculations are considered estimations of the ideal quantity. In this paper they can be identified by the symbol ˆ.

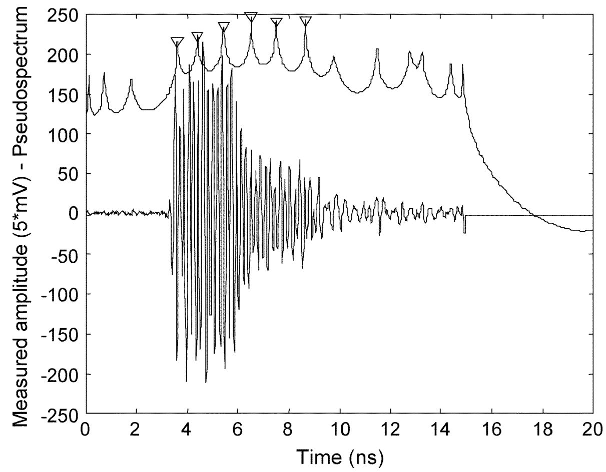

Fig. 1. Measured time-domain response at boresight and MUSIC pseudospectrum. The triangles indicate which patterns were used for reconstruction using signal gating.

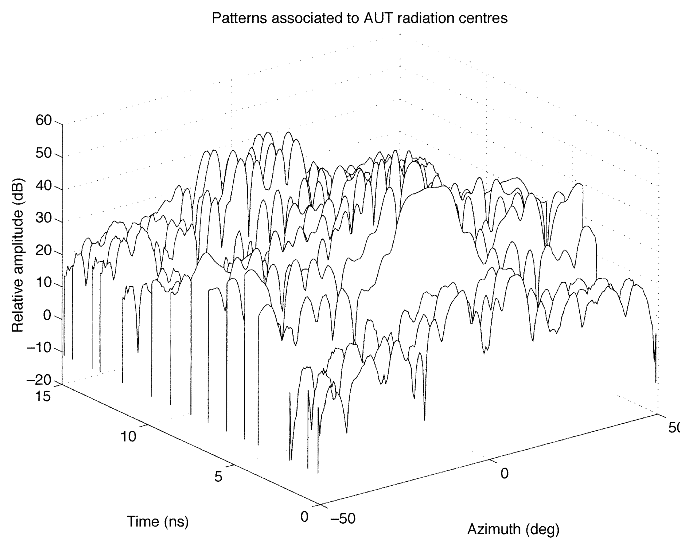

Fig. 2. Representation of the patterns corresponding to the identified radiation centers in the ASAR antenna versus time and azimuth angle.

III. Validation of the Model

For the validation of the model, two completely different antennas are selected: a linear array antenna and a shaped reflector antenna. The array offers the verification of the model for the case of multiple radiation centers, which correspond to its radiating elements, while the shaped reflector shows the capability of this model to group different radiation mechanisms into a single contribution.

The linear array under test is the central subarray of a tile of the Advanced Synthetic Aperture Radar (ASAR) antenna, currently in operation onboard Envisat, an Earth observation mission of the European Space Agency (ESA). The tile is composed of 16 linear subarrays with 24 sequentially rotated, dual linearly polarized annular slots grouped in pairs, and designed to operate at 5.331 GHz with a nominal bandwidth of 16 MHz. The antenna pattern is measured from -50° to 50° in azimuth, every 0.5°.

The second antenna called Eurobeam, is a dual polarized, front fed, shaped reflector designed to operate at 12 GHz onboard the ESA Orbital Telecommunication Satellite. This antenna is extensively used for

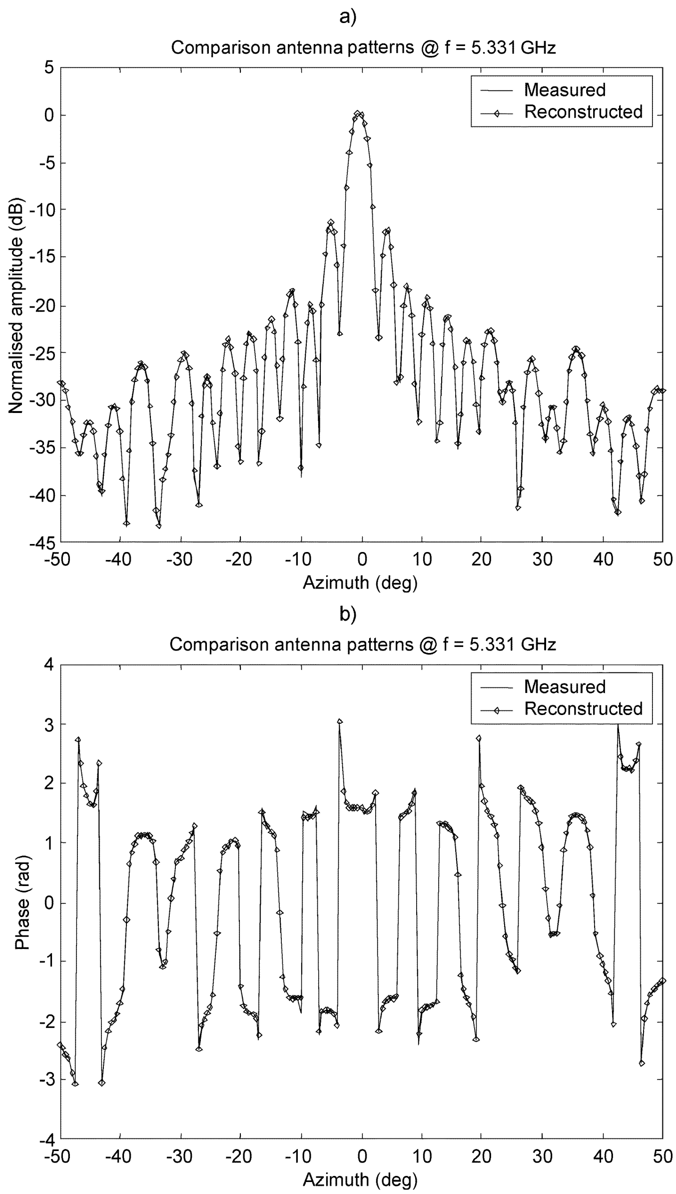

Fig. 3. Comparison between measured and reconstructed patterns of the ASAR antenna at 5.331 GHZ in (a) amplitude and (b) phase.

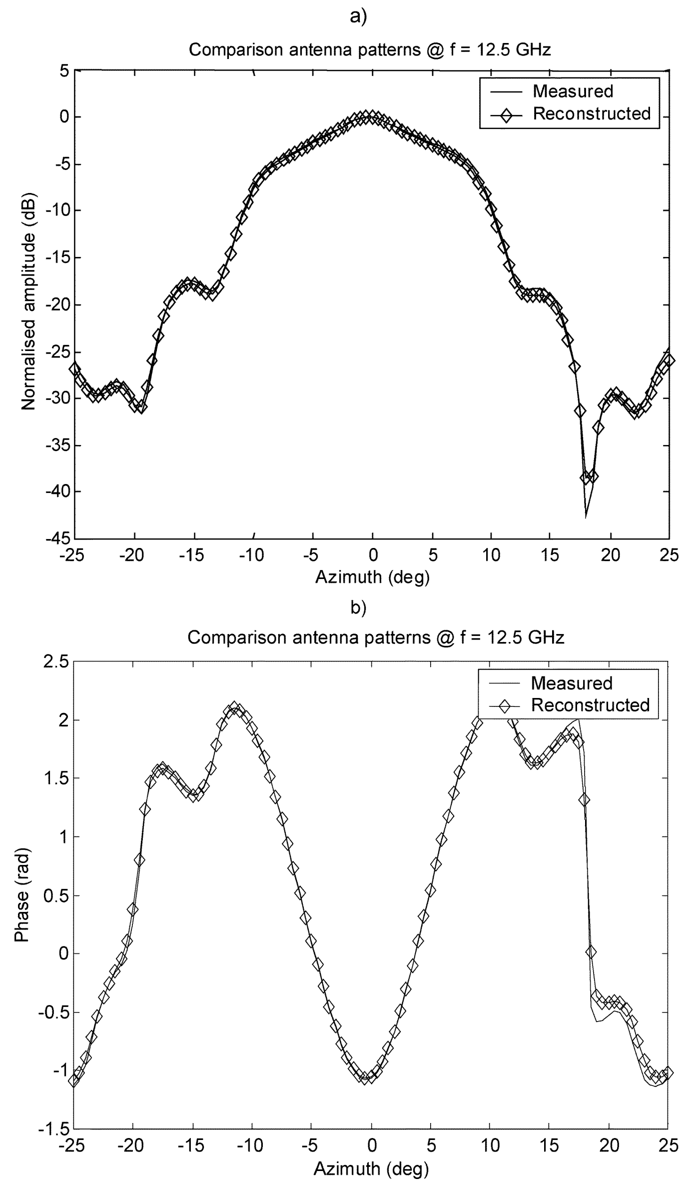

Fig. 4. Comparison between measured and reconstructed patterns of the Eurobeam antenna at 12.5 GHz in (a) amplitude and (b) phase.

range intercomparison. The radiation pattern is measured at 0° elevation from $-25°$ to 25° in azimuth, every 0.5°.

The measurements were made at the ESTEC Compact Antenna Test Range (CATR), which provides a quiet zone of 1.5×2.4 m^2 by a dual cylindrical parabolic reflector configuration. The ASAR patterns are measured with the time-domain instrumentation, where at the transmitting end the range antenna is fed with pulses of 30 V amplitude and 80 ps width, and at the receiving end the antenna under test is connected to a low-noise amplifier followed by a digital oscilloscope, which records time frames of 15 ns duration and 1024 samples. The ESTEC CATR is the first range of its kind validated for time-domain antenna and radar cross-section measurements [12], [13]. The Eurobeam antenna patterns are measured using the standard frequency-domain instrumentation, which is based on a frequency synthesizer and a HP8530 network analyzer. The patterns are recorded for 801 equispaced frequencies over a bandwidth from 2 to 18 GHz.

For the reconstruction of the ASAR measured patterns, the model parameters are retrieved over a bandwidth of 830 MHz around the frequency of operation. It is worth mentioning that the time-domain measurement provided a measurement bandwidth from a few kilohertz to about 20 GHz, and that any other bandwidth could be selected for the reconstruction. Fig. 1 shows the measured time-domain response at boresight and the resultant MUSIC pseudospectrum. At the times coinciding with the most significant maximi of the pseudospectrum (see six triangles in Fig. 1), the complex patterns associated to the radiation centers are estimated. These six patterns plotted in Fig. 2 are added together as in (2) to provide the reconstructed pattern that is depicted in Fig. 3, in both amplitude and phase. One can notice the high degree of reproducibility both in amplitude down to -50 dB and in phase, as shown in the careful reconstruction of all sidelobes and nulls.

The reconstructed patterns of the Eurobeam antenna are retrieved from a 1 GHz bandwidth around 12.5 GHz. The patterns at the central frequency are plotted together with the measured ones in Fig. 4. Again, a high degree of reproducibility is obtained for both amplitude and phase patterns. The reconstruction is achieved using six patterns associated to radiation centers as depicted in Fig. 5.

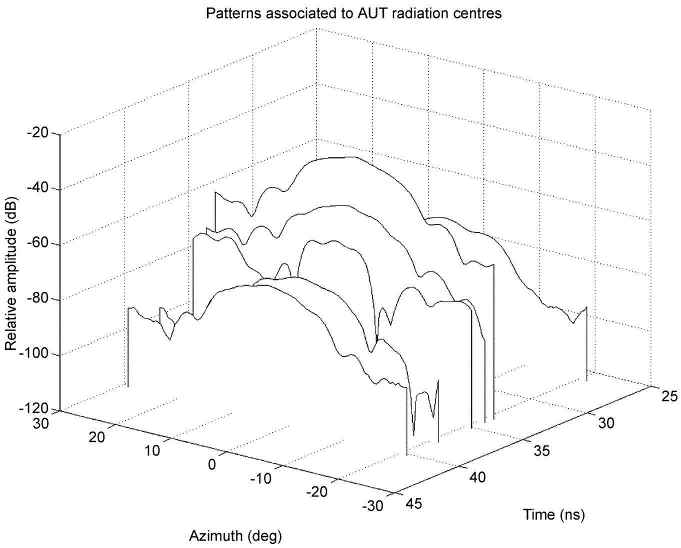

Fig. 5. Representation of the patterns corresponding to the identified radiation centers of the Eurobeam antenna versus time and azimuth angle.

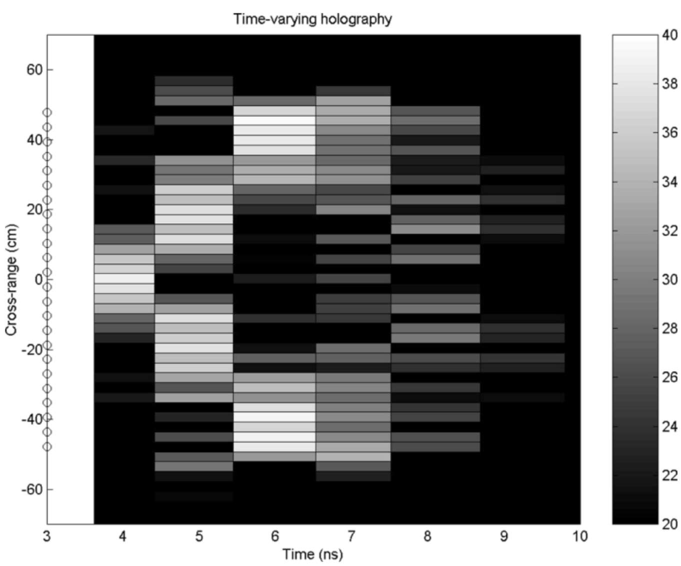

Fig. 6. Time-varying amplitude holography of the ASAR antenna in dB, obtained from the transformation to the near field of the retrieved radiation center patterns. Elements of the array are superimposed on the left Y-axis.

IV. Reconstruction of Time-Varying Aperture Fields

In order to obtain the time-varying holography, each radiation pattern coupled to a radiation center is individually transformed back to the near field as defined in (3). When plotted as a function of their time delay, the time-varying aperture fields appear as depicted in Fig. 6 for the ASAR antenna. In the same figure, the elements of the array are superimposed on the Y-axis to facilitate the interpretation.

In this plot, one can observe several characteristics of the linear array. First, the radiation centers are distributed along the linear array and correspond with groups of array elements, i.e., groups of four, four, and six elements, respectively. In addition, radiation does not occur at the same time in all centers, but it happens sequentially from the center to the ones at the edges, as the feed network of the array excites the different groups of elements. Furthermore, the edge reflection can also be appreciated as a second radiation sequence of lower level but in reverse order.

The time-varying holography also offers the potential to perform nondestructive reverse engineering. Thus, the effective dielectric constant used in the feed-network can be calculated from the apparent effective velocity, which is measured in the plot as the ratio between the time elapsed and distance covered in the array by the maximum aperture field from the center element to the edge ones. In this case, the calculated velocity of 2.65e9 m/s provides an effective dielectric constant of 1.28. This value differs from the design value of 1.14, yielding a difference of approximately 12%.

The lower resolution of the results when compared with the direct time-domain holography in [6], [7] arises from the frequency bandwidth that has been used to generate the plot, i.e., 830 MHz. The result in Fig. 4 and the related interpretation are certainly correct but the bandwidth is limiting the ultimate resolution, being thus a bandpass picture of the electrical behavior of the array. As the bandwidth is further reduced, the picture becomes more "blurred," with fewer radiation centers and more array elements per radiation center. The limit is appreciated in the traditional holography performed at a fixed frequency, which does not allow to appreciate any timely variation of the aperture fields at all. At the other extreme, the direct time-domain holography contains all features of the antenna, because of the large bandwidth considered, and the number of radiation centers coincides with the number of elements pairs in the array.

V. Conclusion

A model to reconstruct measured antenna patterns in compact ranges has been presented and illustrated with experimental results from two space antennas. The patterns can be acquired with frequency- or time-domain instrumentation, provided in the former that at least measurements are taken over a certain bandwidth. The model parameters are the number of radiation centers of the antenna under test, their associated measured complex pattern and their time delay. Furthermore, the retrieved patterns from the radiation centers can be individually transformed to the near field, and when plotted as a function of their time delay they provide a time-varying holography of the antenna. This is a new approach to the direct time-domain holography. The resultant holography shows those features that are contained in the bandwidth considered for the reconstruction.

Acknowledgment

The authors wish to thank the independent reviewers for their comments and also Dr. G. Toso for the fruitful discussions held on this topic.

References

[1] L. B. Felsen, *Transient Electromagnetic Fields, Chapter 4: Radiation and Reception of Transients by Linear Antennas*. Berlin, Germany: Springer-Verlag, 1976.

[2] E. K. Miller, "An exploration of radiation physics in electromagnetics," in *IEEE Int. Symp. Antennas Propagation Soc.*, vol. 3, July 1997, pp. 2048–2051.

[3] H. G. Schantz, "Electromagnetic energy around Hertzian dipoles," in *IEEE Int. Symp. Antennas Propagation Soc.*, vol. 2, 1999, pp. 1320–1323.

[4] C. Ozdemir, R. Bhalla, and H. Ling, "A radiation center representation of antenna radiation patterns on a complex platform," *IEEE Trans. Antennas Propagat.*, vol. 48, no. 6, pp. 992–1000, June 2000.

[5] T. H. Lee and W. D. Burnside, "A diagnostics technique used to obtain cross-range radiation centers from antenna patterns," *IEEE Trans. Antennas Propagat.*, vol. 37, pp. 1242–1249, Oct. 1989.

[6] J. Marti-Canales and L. P. Ligthart, "Time domain antenna holography," *IEE Electronic Letters*, vol. 36, no. 6, pp. 493–494, Mar. 2000.

[7] J. Martí-Canales and L. P. Ligthart, "Method and system for time domain antenna holography," U.S. Patent 6 469 672 B1, Oct. 22, 2002.

[8] R. O. Schmidt, "Multiple emitter location and signal parameter estimation," *IEEE Trans. Antennas Propagat.*, vol. 34, pp. 276–280, Mar. 1986.

[9] J. Marti-Canales and L. P. Ligthart, "Modeling and pattern error correction of time domain far-field antenna measurements," *Proc. Inst. Elect. Eng. Microwaves, Antennas Propagat.*, vol. 148, no. 2, pp. 133–136, Apr. 2001.
[10] D. Spielman, A. Paulraj, and T. Kailath, "Performance analysis of the MUSIC algorithm," in *Proc. IEEE ICASSP*, Tokyo, 1986, pp. 1909–1912.
[11] S. U. Pillai and B. H. Kwon, "Forward/backward spatial smoothing techniques for coherent signal identification," *IEEE Trans. Acoust., Speech, Signal Proc.*, vol. 37, pp. 8–15, Jan. 1989.
[12] J. Marti-Canales, L. P. Ligthart, and A. G. Roederer, "Performance analysis of a compact range in the time domain," *IEEE Trans. Antennas Propagat.*, vol. 50, pp. 511–516, Apr. 2002.
[13] R. V. de Jongh, J. Marti-Canales, and L. P. Ligthart, "Analysis of time domain RCS measurements in compact ranges," *Electron. Lett.*, vol. 36, no. 24, pp. 1986–1987, Nov. 23, 2000.

An Ultrawide-Band Impedance-Loaded Genetic Antenna

Edward E. Altshuler and Derek S. Linden

***Abstract*—There are many new radar and communications systems that will utilize ultrawide-band antennas. In this investigation, a compact genetic antenna consisting of a set of wires connected in series and with impedance loads is designed and measured. The shape of the antenna and the location of the loads and their impedances are optimized using a genetic algorithm. The resultant antenna is mounted over a ground plane and has elliptical polarization and near hemispherical coverage. It has a VSWR that is under about 4.5 over the 50 to 1 band from 300 to 15000 MHz. The VSWR, radiation patterns and antenna efficiency have been simulated and the VSWR has been measured.**

***Index Terms*—Genetic algorithm, impedance-loaded antenna, ultrawide-band antenna.**

I. Introduction

One of the most challenging antenna problems is the ultrawide-band (UWB) antenna. From a qualitative standpoint UWB has been assumed to signify large relative bandwidth signals [1]. UWB has been used in the time domain for systems that radiate very narrow time-width pulses and in the frequency domain for wideband communications and radar systems; our investigation addresses the frequency domain. One approach for obtaining wide bandwidths is to insert lumped impedances in the antenna structure. Probably the first impedance-loaded wide-band linear antenna was reported by Altshuler [2]. He placed a resistive load about 1/4 wavelength from the end of a monopole over a ground plane and was able to obtain a VSWR under 2.5 over a 3 to 1 band. Wu and King [3] then showed that with a properly tapered resistance along the antenna, it was possible to produce an outward traveling wave and thus a nearly frequency independent antenna. Shen [4] approximated the continuously resistive loaded antenna with a linear step function resistance and built and tested this antenna. Using the Wu and King approach, Lally and Roach [5] built and tested a continuously resistive loaded antenna and measured it over a 100 to 1 band. More recently, Boag *et al.* [6] used a genetic algorithm (GA) to design a UWB monopole; the algorithm was used to determine the locations and impedances of the inserted loads. They achieved satisfactory performance over a 15 to 1 band. The previous loaded antennas were monopoles; the shortest had an electrical length of about 0.2λ at the lowest frequency.

In this investigation, a more compact antenna consisting of a set of wires connected in series is designed. The shape of the antenna and the location of the loads and their impedances are determined by the GA, hence it is called a genetic antenna. Prior research on this antenna can be found in [7]–[10]. We show that satisfactory results can be obtained by using loads that consisted of a resistor in parallel with an inductor. The addition of a capacitor was considered, however it was not used since it did not result in a significant improvement in antenna performance and also would have complicated the fabrication of the antenna. The antenna is enclosed in a cube of less than 0.1λ on a side at the lowest frequency and mounted over a ground plane. In addition to the antenna being more compact, it also has the advantage of having an elliptically polarized radiation pattern and near hemispherical coverage. The optimization is done using the GA in conjunction with the Numerical Electromagnetics Code (NEC-4) [11]. The initial design was done for the frequency band from 300 to 6000 MHz; this was later extended to 15 000 MHz. All computations were done for the antenna over an infinite ground plane.

Manuscript received December 27, 2002; revised December 1, 2003. This work was supported in part by the Air Force Office of Scientific Research (AFOSR) and in part by the Defense Advanced Research Projects Agency (DARPA).
E. E. Altshuler is with the Sensors Directorate, AF Research Lab, Hanscom Air Force Base, Hanscom AFB, MA 01731 USA (e-mail: edward.altshuler@hanscom.af.mil).
D. S. Linden is with Linden Innovation Research, Ashburn, VA 20146-1601 USA (e-mail: dlinden@lindenir.com).
Digital Object Identifier 10.1109/TAP.2004.834468

II. Approach

A. Computations

To begin the GA process, a cost function, which contains the characteristics to be optimized, must first be defined; for this investigation we only optimized the VSWR. The fitness function we used was

$$\text{Score} = \sum_{\text{all frequencies}} \begin{cases} 0.25(\text{VSWR}-1) & \text{if VSWR} < 3.0 \\ (\text{VSWR}-2)^5 & \text{if VSWR} \geq 3.0. \end{cases}$$

Each antenna was tested at the following twelve frequencies: 6000, 5400, 4800, 4200, 3600, 3000, 2400, 1800, 1200, 600, 450, and 300 MHz.

We next had to identify a search space of possible antenna configurations. We chose a design space that consisted of a cube of height h/λ; all the possible vertices of the wires that are to be connected to form the antenna are within this volume. The GA used floating point numbers to specify three-dimensional (3-D) wire coordinates, so a virtually continuous range of values was possible for each coordinate value within the constraints of the cube. We also specified the number of wire segments used in each design. Through experimentation, we have found that using five–eight segments tends to give enough degrees of freedom to the GA to allow it to produce interesting designs. In this case, six segments worked best.

The GA randomly selects a sample population of wire configurations. Ideally, the size of this sample should be large enough so that a wide selection of possible configurations is included, yet not too large such that computation time becomes unnecessarily long. We used a population size of 70 for our optimization, and a value of 8.5 cm for h. Each antenna configuration of the sample population